Journal Pre-proof

Different melt source regions for the volcanics of the bushveld large igneous province: New observations from MELTS modeling of the palaeoproterozoic Rooiberg Group (South Africa)

Olutola O. Jolayemi, Laurence Robb, Nils Lenhardt, Hannah S.R. Hughes

PII: S1464-343X(20)30250-8

DOI: https://doi.org/10.1016/j.jafrearsci.2020.103999

Reference: AES 103999

To appear in: *Journal of African Earth Sciences*

Received Date: 8 June 2020

Revised Date: 30 July 2020

Accepted Date: 26 August 2020

Please cite this article as: Jolayemi, O.O., Robb, L., Lenhardt, N., Hughes, H.S.R., Different melt source regions for the volcanics of the bushveld large igneous province: New observations from MELTS modeling of the palaeoproterozoic Rooiberg Group (South Africa), *Journal of African Earth Sciences* (2020), doi: https://doi.org/10.1016/j.jafrearsci.2020.103999.

Different melt source regions for the volcanics of the Bushveld large igneous province: New observations from MELTS modeling of the Palaeoproterozoic Rooiberg Group (South Africa)

Olutola O. Jolayemi[1]*, Laurence Robb[1,2,5], Nils Lenhardt[3,5], Hannah S.R. Hughes[4,1]

[1]School of Geosciences, University of the Witwatersrand, Private Bag 3, 2050 Johannesburg, South Africa
[2]Department of Earth Sciences, University of Oxford, South Parks Road, OX1 3AN Oxford, United Kingdom
[3]Department of Geology, University of Pretoria, Private Bag X20, 0028 Pretoria, South Africa
[4]Camborne School of Mines, College of Engineering, Mathematics and Physical Sciences, University of Exeter, Penryn TR10 9FE, United Kingdom
[5]DSI-NRF CIMERA, University of Johannesburg, Johannesburg, South Africa

* Corresponding author:
School of Geosciences,
University of the Witwatersrand,
Private Bag 3,
Johannesburg 2050,
South Africa
Tel.: +27 (0) 735 252 385
E-mail: olutola.j@gmail.com

Manuscript to be submitted to
Journal of African Earth Sciences

Revised Version: 30 July 2020

Different melt source regions for the volcanics of the Bushveld large igneous province: New observations from MELTS modeling of the Palaeoproterozoic Rooiberg Group (South Africa)

Abstract

The volcanic Rooiberg Group represents the extrusive phase of the Bushveld Magmatic Province in South Africa, forming the roof as well as the floor of the mafic-ultramafic 2057 Ma Rustenburg Layered Suite. Typically, the volcanic rocks of the Rooiberg Group vary from mafic compositions in the oldest unit (the Dullstroom Formation) to felsic compositions in the younger overlying units (the Damwal, Kwaggasnek and Schrikkloof formations). The lower parts of the Dullstroom Formation (including a basal rhyolitic unit) occur beneath the Rustenburg Layered Suite (RLS) in the southeastern part of the Bushveld Province, whereas the remainder of the Rooiberg Group occurs above the RLS. In this study, petrographic descriptions, whole rock geochemistry and MELTS modeling are used to show that the Dullstroom rhyolite could have evolved from fractional crystallization of a siliceous and magnesian mafic liquid such as the so-called B1 liquid, parental to the lower parts of the Rustenburg Layered Suite. Due to its unique position at the base of the otherwise andesitic to dacitic Dullstroom Formation, the focus of this contribution is on the Dullstroom rhyolite and a comparison thereof with the rhyolites of the upper formations. Consistent with previous studies, the new data generated in this study show that a clear distinction can be made between the rhyolite in the Dullstroom, and those of the Damwal, Kwaggasnek and Schrikkloof formations. The Dullstroom rhyolite exhibits higher MgO contents (1.41-1.87 wt%) compared to the distinctly ferroan rhyolites of the Damwal, Kwaggasnek and Schrikkloof formations (0.01-0.91 wt% MgO). Similarly, immobile trace elements such as Y and Nb range from 9.72 to 12.7 ppm and 4.43 to 4.53 ppm, respectively, for the Dullstroom rhyolite, and are significantly different to the upper rhyolites (Y - 12.6-87.2 ppm and Nb - 12.3-24.2 ppm) suggesting likely petrogenetic differences.

MELTS modeling shows that the Dullstroom rhyolite could not have evolved from the same liquids that generated the rhyolites of the Damwal, Kwaggasnek and Schrikkloof formations. The modeling suggests that the Dullstroom rhyolite formed through ~20% assimilation of upper continental crustal rocks during fractional crystallization of the B1 composition, and not from the low-Ti basaltic andesite, as previously proposed for the overlying rhyolites. The modeling aspects of this study provide evidence for different sources and melting-fractionation pathways throughout the evolution of the Bushveld Magmatic Province, consistent with characteristics recorded by the volcanic edifice of this large igneous province.

Keywords: Bushveld Magmatic Province; Rhyolite; MELTS modeling; Geochemistry; South Africa; Kaapvaal Craton.

1. Introduction

The world-renowned and economically important Palaeoproterozoic Bushveld Magmatic Province (BMP) is located in northeastern South Africa on the Kaapvaal Craton (Fig. 1). It was described as a large igneous province (LIP) by Ernst and Buchan (2001) and consists of more or less coeval intrusive and extrusive rocks. The intrusive parts are predominantly composed of the mafic Rustenburg Layered Suite, the Rashoop Granophyre Suite and the Lebowa Granite Suite. In addition, more recently, the Molopo Farms Layered intrusion, Okwa basement complex intrusions, and smaller intrusions of the Bushveld high-Ti suite near the Vredefort impact complex, are usually included as parts of the larger BMP (Reichardt, 1994; Kinnaird, 2005; Mapeo et al., 2006; Lenhardt and Eriksson, 2012). The volcanism that preceded the intrusive activity is represented by the Rooiberg Group (Lenhardt and Eriksson, 2012).

Despite more than a century of mining and academic research on the BMP, there remain many questions regarding the chemical as well as chronological relationships between its individual units such as the volcanics, granophyres and granites. This contribution focuses on the volcanic Rooiberg Group and the petrogenesis of the lowermost unit, which comprises both mafic volcanics and rhyolite. Petrographic comparisons will be conducted between the rhyolite at the base of the Rooiberg Group and those that occur higher in the succession. Albeit the Rooiberg Group consists of magnesian and feroan lavas (Twist, 1985; Twist and Hammer, 1987; Mathez et al., 2013), the magnesian lavas are compositionally distinct in comparison to the ferroan lavas (eg. Twist, 1985; Mathez et al., 2013). In stratigraphic order, the Rooiberg Group can be divided into the Dullstroom, Damwal, Kwaggasnek and Schrikkloof formations (Fig. 2). There is still uncertainty regarding the petrogenesis of the Dullstroom Formation and its relationship to the overlying formations. Mathez et al. (2013) hypothesized that the ferroan felsic lavas of the Damwal, Kwaggasnek, and Schrikkloof formations formed by fractional crystallization of a mafic liquid, but showed that they are petrologically unrelated to the lavas of the Dullstroom Formation. Exactly how the latter could have formed remained problematic. Accordingly, this contribution aims to provide more clarity on the petrogenesis of the so-called Basal Rhyolite of the Dullstroom Formation (Hatton and Schweitzer, 1995; Schweitzer et al., 1995). The Basal Rhyolite is of interest because it is magnesian, by comparison with the rhyolites of the overlying Damwal, Kwaggasnek and Schrikkloof formations, which are all ferroan. The term Basal Rhyolite will not be used in this work to describe the rhyolites that occur at the base of the Dullstroom Formation and instead, we will use the term Dullstroom rhyolite to describe the latter.

The Dullstroom rhyolite occurs beneath the dominant low-Ti basaltic andesite magma composition of the Dullstroom Formation and appears to be a petrogenetic oddity. We compare the rhyolite in the Dullstroom Formation with the rhyolites of the younger formations in order to establish if all the rhyolites in the Rooiberg Group represent the same package of volcanism from their melt source(s). By also comparing geochemical trends and modeled melt compositional constraints, this is used to ascertain whether the rhyolite at the base of the Dullstroom Formation is consistent with the onset of Bushveld volcanism. Modeling is conducted using the MELTS program of Ghiorso and Gualda (2015) and by computing the continuity of liquid lines of descent.

2. Geological Setting

Within the BMP, the volcanic Rooiberg Group lies unconformably above the volcano-sedimentary sequence of the Pretoria Group (Fig. 2) that forms the upper part of the Transvaal Supergroup (Cheney and Twist, 1991; Lenhardt et al., 2017). The rocks of the Rooiberg Group attain a volume of approximately 200,000-300,000 km^3 (Twist and French, 1983), making it one of the largest accumulations of silicic volcanic rocks on Earth (Twist and French, 1983; Harmer and Armstrong, 2000; Lenhardt et al., 2017). The estimated age for the Rooiberg Group ranges from 2061±2 Ma (Walraven, 1997) to 2057.3±3.8 Ma (Harmer and Armstrong, 2000). This age range suggests that the volcanic rocks were erupted prior to both the Rustenburg Layered Suite (now dated at 2055.9±0.3 Ma to 2054.8±0.3 Ma; Zeh et al., 2015, 2056.88 ± 0.41 Ma; 2057.04 ± 0.55 Ma; revised from Scoates and Friedman, 2008; Scoates and Wall, 2015, 2057.64 ± 0.69 Ma; Maier et al., 2018) as well as the Lebowa Granite Suite (dated at 2054±2 Ma; Walraven and Hatting, 1993) and the Rashoop Granophyre Suite (dated at 2053±12 Ma; Coertze et al., 1978). The possibility of an overlap between the ages of the Rooiberg Group and intrusive phases of the BMP cannot however be ruled out because the Rooiberg Group is incompletely dated, especially in its upper reaches. In addition, Buchanan et al. (2004) presented a crystallization age of 2071 +94/-65 Ma for units of the Dullstroom (and Damwal) Formation, which highlights the uncertainty regarding the timing of Dullstroom Formation emplacement relative to the Rustenburg Layered Suite. Another evidence of overlap and uncertainty was presented by Worst (1944) and von Gruenewaldt (1968) who observed that the felsite was in place prior to the consolidation of the Main and Upper zones of the intrusive Rustenburg Layered Suite.

The lowermost Dullstroom Formation, forming the focus of this contribution, occurs only in the southeastern part of the Rooiberg Group (Fig. 1), lying unconformably over Pretoria Group sedimentary rocks (Twist, 1985; Cheney and Twist 1991; Mathez et al., 2013) and beneath Bushveld intrusive lithologies (Eriksson et al., 1995). Generally, the lower Dullstroom Formation is characterized by an approximately 2 km thick sequence of volcanic rocks, predominantly ranging in composition from basalt to andesite with thin laterally continuous sedimentary units (Eriksson et al., 1994; Schweitzer et al., 1995; Buchanan et al., 1999, 2004). Within the mapped area, the lowermost unit of the Dullstroom Formation, lying directly on top of the Pretoria Group, is the Dullstroom rhyolite, reaching thicknesses of ~200 m (Fig. 3). The Dullstroom rhyolite is overlain by a more dominant, ~600 m thick, basaltic andesite (i.e. the low-Ti basaltic andesite (LTI) of Hatton and Schweitzer, 1995; Schweitzer et al., 1995; Buchanan et al., 1999). The basaltic andesite alternates with andesite (~400 m thick) and rhyodacite (~500 m thick), leading to a succession that becomes more silicic towards the top of the formation. The upper part of the Dullstroom Formation, together with the other three formations of the Rooiberg Group, forms the roof of the intrusive Rustenburg Layered Suite (Hatton and Schweitzer, 1995; Schweitzer et al., 1995). The rhyolites of the three younger formations (Damwal, Kwaggasnek and Schrikkloof) are best exposed in the Loskop Dam area north of Middleburg in Mpumalanga (Fig. 1). Here, the Rooiberg Group exhibits a thickness of ~3,500 m (Twist, 1985; Clubley-Armstrong, 1977; Lenhardt et al., 2017). The Damwal Formation in this area is primarily composed of dacites, rhyodacites, and a variety of siliciclastic sedimentary interbeds, while the overlying Kwaggasnek Formation is dominated by rhyolites with minor rhyodacites and dacites. The Schrikkloof Formation is composed of intercalations of rhyodacite with rhyolites and dacite at the base (the lower 1000 m), while becoming more rhyolitic towards the top (see Lenhardt et al. (2017) for more detailed descriptions of the stratigraphy).

A range of field, petrographic and geochemical analyses show that the eruptional as well as depositional processes responsible for the formation of the Damwal, Kwaggasnek and Schrikkloof formations appear to be significantly different to those that led to the development of the underlying Dullstroom Formation. Mapping of the lower Dullstroom Formation near its type locality (Jolayemi, 2015) has shown that this formation is characterised by a sequence of lava flows, ranging in composition from rhyolite at the base to basalt and subordinate dacite towards its stratigraphic top. Internally, the Dullstroom rocks all appear massive and contain a variety of idiomorphic phenocrysts, set in a cryptocrystalline matrix (see Section 4 on lithology and petrography). Due to their composition, extent and distribution, the rocks can generally be described as sheet lavas.

Recent observations on the Damwal, Kwaggasnek and Schrikkloof formations by Lenhardt et al. (2017), however, have revealed that these rocks are not related to lava flows as previously thought (Twist and French, 1983; Schweitzer et al., 1995). Instead, Lenhardt et al. (2017) show that the upper formations typically exhibit an absence of a continuous basal autobreccia, which is normally taken as a sign of a rhyolitic lava flow. Furthermore, many samples exhibit remnant vitroclastic textures (glass shards) with fabrics ranging from eutaxitic (shard-like material) to parataxitic (flow bands). Observed kinematic indicators within these formations include oblique and sheath folds (reflecting ductile deformation under shear stress), fabric imbrication, and boudinaged fiammé (Lenhardt et al., 2017). All these provide evidence for an origin from high-temperature (rheomorphic) to very high-temperature (lava-like) ignimbrites (Lenhardt et al., 2017), resembling the Snake River-type rhyolites of Branney et al. (2008). At Loskop Dam, the ignimbrites of the upper formations are intercalated with a range of siliciclastic sediments and peperites that formed due to the interaction and concomitant sedimentation of ignimbrites with these sediments (Lenhardt and Eriksson, 2012; Lenhardt et al., 2017). This provides evidence for a dynamic depositional environment entailing interaction of the products of highly explosive eruptions with siliciclastic 'background sedimentation'. Thus, there is a shift from the effusive lava-like eruptions of mafic magmas in the lower units of the Rooiberg to increasingly explosive, sub-aerial volcanism and deposition of felsic pyroclastic rocks in the upper units of the Rooiberg Group.

For the more mafic Dullstroom Formation lavas, fissure vents appear to be the most likely magma conduit (cf. Manley, 1996). On the other hand, an origin from major caldera features (cf. Moore and Kokelaar, 1998) or fissure eruptions (cf. Fernandez et al., 2011) appear likely for the younger formations. However, limited field evidence has been observed for either calderas or fissures within the Rooiberg Group. Vent sites, however, could have been buried by caldera-fill deposits, emplaced in the course of eruptions during caldera subsidence or obscured by later tectonism and erosion (Bryan et al., 2002; White et al., 2009). One likely vent site for Rooiberg-related volcanism is the Vergenoeg Igneous Complex (VIC) near Rust de Winter (Limpopo Province) which represents a terminal eruptive phase of the Rooiberg Group erupted on top of the Schrikkloof Formation and immediately preceding Waterberg Group deposition (Borrok et al., 1998). The relationship between the VIC and the Rooiberg Group is currently being investigated.

3. Sampling locations, materials and methods

Within the sampling area, the volcanic succession of the lower Dullstroom Formation reaches a total thickness of approximately 1500 m. A stratigraphic section of the study area is shown in Fig. 3. Samples used in this study were obtained in the area near Dullstroom (S25°23’0”, E30°0’0”) in the eastern part of the Bushveld Province where the lower Dullstroom Formation is exposed. All other rhyolites were taken from the younger formations in the Loskop Dam area (S25º25’17.8”, E29º31’39.0”) for comparative purposes. Based on location and apparent freshness, 23 samples were collected from the lower Dullstroom Formation for petrographical and geochemical analysis. Furthermore, 41 samples representing the younger formations, i.e. the Damwal, Kwaggasnek and Schrikkloof formations from the Loskop Dam area were used for comparison. All samples were carefully selected, avoiding those characterized by vesicles and amygdales, as well as alteration.

X-ray fluorescence (XRF) analysis for major element oxides was conducted at the University of Pretoria and a selection of trace elements were analysed using inductively coupled plasma mass spectrometry (ICP-MS) at the University of Cape Town (see Table 1).To help determine the degree of alteration, the chemical index of alteration (CIA) was calculated using the formula Al_2O_3 / (Al_2O_3 + CaO + Na_2O + K_2O) x100 according to Nesbitt and Young (1982). The CIA accounts for the extent to which feldspars have been altered to aluminous clay and hence is used as a tool in estimating the degree of chemical alteration of rock samples. For example, illite and montmorillonite have CIA values that range between 75 and 85, indicating a more intense weathering whereas unaltered basaltic rocks usually have CIA values between 30 and 45.

Petrogenetic modeling was carried out using the MELTS program (Ghiorso and Gualda, 2015), assuming that the Rooiberg Group samples represent primary liquid compositions and that the effects of subsequent alteration were minor. Major element oxide contents of possible parental liquids were used to establish liquid lines of decent that best resemble the Dullstroom rhyolite composition. The initial parental magma compositions used in the modeling are from Barnes et al. (2010) – B1, B2, B3 – described as parental to the formation of the Rustenburg Layered Suite of the BMP. Other parental liquids modeled include the low-Ti basaltic andesite (LTI), previously suggested to be the parental magma of the Rooiberg Group as a whole (Buchanan et al., 1999, 2002; Günther et al., 2018). MELTS modeling involved isobaric calculations with a 10ºC interval decrease as crystallisation occurred between a maximum of 1400ºC and a minimum of 800ºC. Parameters used in the MELTS model are displayed in Table 2. The model assumes assimilation and fractional crystallization (AFC) type processes by incorporating a mass of assimilant at each cooling step, while simultaneously fractionally crystallising a realistic cumulus assemblage and calculating the residual liquid composition.

4. Lithology and petrography

The lithologies briefly described in this section include the rhyolites present in the Dullstroom, Damwal, Kwaggasnek and Schrikkloof formations of the Rooiberg Group.

The Dullstroom rhyolite is reddish brown to grey in colour and may appear massive (Fig. 4a) or with localized strong flow-banding. This unit exhibits a microcrystalline groundmass with no visible phenocrysts.

The Damwal rhyolite appears reddish brown, aphanitic and contains some phenocrysts (Fig. 4b). The microcrystalline groundmass is mainly composed of plagioclase (~4 vol.%), quartz (~4 vol.%) and minor K-feldspar (~5 vol.%) while phenocrysts (<5 vol.%) include plagioclase, quartz and K-feldspar and all range between 0.1- 0.5 μm in size. Minor phases such as hornblende, chlorite, muscovite and some Fe-Ti-rich minerals (ilmenite) are also present. These samples also exhibit vesicles and amygdales that are about 2-3 vol.% with diameters that are usually <3 cm.

The samples representing the Kwaggasnek rhyolite (Fig. 4c) show a plagioclase and quartz dominated microcrystalline groundmass and flow-banding on outcrops is more pronounced in this unit than in the Damwal rhyolites. Phenocrysts are present in minor amount (2-5 vol.%) and are mainly plagioclase (~0.5 μm) and quartz (0.1-0.5 μm) while hornblende and chlorite (±muscovite) occur as accessory phases. Few vesicles are locally present, some of these as amygdales, filled with secondary minerals such as quartz and chlorite. Spherulites in the Kwaggasnek rhyolite can reach 3 cm in diameter and are made up of quartz and K-feldspar. The majority of the spherulites have developed into lithophysae.

The Schrikkloof rhyolite (Fig. 4d) exhibits a microcrystalline to cryptocrystalline groundmass that is composed of quartz and feldspars. Phenocrysts in these samples include quartz, plagioclase and feldspar, although these occur in minor amounts compared to the Kwaggasnek and Damwal rhyolites. These samples show more physical evidence of alteration than the Damwal and Kwaggasnek Formations, such as the presence of clay minerals like illite.

5. Geochemistry

5.1 Major element oxides geochemistry

The loss on ignition (LOI) values of the samples used in this study have an average of 1.72 wt%. The average value for the chemical index of alteration (CIA) (Nesbitt and Young, 1982) is 58.02 for all the samples used in this study, and all highly altered samples were excluded from the study.

To explore the possible origin of the rhyolites within the Rooiberg Group, we employ the classification plots of Frost et al. (2001) (Fig. 5). The classification plots include the modified alkali-lime index (MALI) which is used to decipher the abundance and composition of feldspar (Fig. 5a), the Fe-index which is used to decipher the magma differentiation history (Fig. 5b), and the aluminium saturation index (ASI) which is used to show the distinction between peraluminous and metaluminous rocks (Fig. 5c). Frost et al. (2001) showed that these classification schemes provide evidence that a variation in composition and pressure can yield different melt compositions that are different to one another, such as distinguishing ferroan lavas from magnesian types. They also proposed that the composition of a liquid can be used to decipher the most probable composition of the source melt, as employed in this work.

5.1.1 Geochemical comparison of the rhyolites within the Rooiberg Group

All Dullstroom rhyolites are magnesian, calcic and weakly peraluminous (Fig. 5), in contrast to the rhyolites observed in the upper formations that include the Damwal, Kwaggasnek and Schrikkloof formations. The rhyolites in the upper formations are ferroan, calc-alkalic to alkali-calcic and mainly metaluminous. These results are similar to those shown in Mathez et al. (2013), who described the rhyolites of the Kwaggasnek and Schrikkloof formations as weakly to moderate peraluminous rather than metaluminous. It is important to state that the weakly peraluminous composition of the Dullstroom rhyolite might be construed to suggest that these rocks are products of the melting of an alumina-rich source, such as a metasediment, resulting in similarity to S-type granites. This is not the case for the Dullstroom rhyolites, however, as their position in the plot (Fig. 5) is a function of their fractionation history. The Fe_2O_3 content of the ferroan rhyolites range between 1.11-7.37 wt.% while that of the Dullstroom rhyolite show a range between 3.72-4.33 wt.%. Although the ferroan rhyolites differ slightly from the magnesian Dullstroom rhyolite in their aluminosity, other elemental compositions reveal more distinct differences. We propose that the main difference between the Dullstroom rhyolites and those of the upper formations (SiO_2> 70%) can be observed in the MgO and CaO compositions, similar to the observation of Mathez et al. (2013). The MgO and CaO compositions of the Dullstroom rhyolites are 1.41-1.87 wt.% and 1.96-3.09 wt.%, respectively. On the other hand, the rhyolites of the upper formations show MgO and CaO compositions that are lower, at 0.08-0.91 wt.% and 0.00-1.56 wt.%, respectively.

5.1.2 Trace element geochemistry

Trace element signatures normalized to the bulk continental crust composition of Rudnick and Gao (2003) are displayed in Fig. 6, and show a comparison between the Dullstroom rhyolites and the rhyolites of the upper formations. Evident from the plot is the difference between the trend exhibited by the Dullstroom rhyolite compared to the Damwal, Kwaggasnek and Schrikkloof rhyolites. The Dullstroom rhyolite is compositionally similar to the bulk continental crust, a trend also identified by Mathez et al. (2013) who pointed out that the Dullstroom rhyolite (1.41-1.87 wt.% MgO; Table 1) is more similar to the magnesian lavas of the Dullstroom Formation (1.8-6.17 wt.% MgO; Table 1) than to the rhyolites of the upper formations (0.01-0.91 wt.% MgO). Other notable differences include lower Rb (87.85-126.46 ppm) and Th (3 ppm) contents in the Dullstroom rhyolite, while the rhyolites of the upper formations (52.2-212 ppm Rb; 9.68-35.1 ppm Th) show significant enrichment (Table 1). Enhanced Ba (903.42-1534.07 ppm) contents can be seen for the Dullstroom rhyolite whereas the rhyolites of the upper formation are more depleted (198-1197 ppm Ba). Furthermore, the rhyolites of the upper formations show much lower V (0.19-46.2 ppm) and Cr (0.38-60.7 ppm) contents than the Dullstroom rhyolite (53.21-54.21 ppm V; 130.09-135.71 ppm Cr).

6. MELTS modeling

In order to constrain the parental magma and liquid compositional trend for the Dullstroom rhyolite, the MELTS modeling algorithm, after Ghiorso and Gualda (2015), was employed. MELTS modeling was used to calculate the major element liquid lines of decent for likely parental magma compositions, both in fractional crystallisation (FC) and assimilation with fractional crystallisation (AFC) modes. Various initial magma compositions ranging from the Bushveld 1 (B1), Bushveld 2 (B2) and Bushveld 3 (B3) magmas, all interpreted as different parental magmas to the mafic units of the Rustenburg Layered Suite (Barnes et al., 2010), were modeled to determine the origin of the Dullstroom rhyolite. These melts represent the compositions interpreted by Barnes et al. (2010) as parental to the Lower and lower Critical zones (B1), the upper Critical Zone (B2) and the Main Zone (B3) of the RLS. Furthermore, VanTongeren et al. (2010) and Mathez et al. (2013) also suggested that escaped intercumulus liquids from the upper Main Zone and Upper Zones of the Rustenburg Layered Suite might represent the source of the Rooiberg Group ferroan rocks. In addition, the average low-Ti basaltic andesite liquid, suggested as parental to the rhyolites of the upper Damwal, Kwaggasnek and Schrikkloof formations (Buchanan et al. 2002; Günther et al., 2018) was also modeled as a starting composition to determine if the origin of the Dullstroom rhyolite might be of low-Ti composition, such as considered possible for the upper Rooiberg formations (Buchanan et al., 1999, 2002; Gunther et al., 2018).

Details of the MELTS parameters are shown in Table 2. No fractionation results were generated or completed at a pressure less than 2.5 kbar. The low pressure values (2-4 kbar) utilized in our MELTS model is similar to those of Günther et al. (2018) that range from 2 to 4.5 kbar, obtained from minerals representing mafic lavas of the Dullstroom Formation. These low pressure values are consistent with the suggested shallow crustal depth of crystallization (Günther et al., 2018) for the evolution of the Rooiberg Group and accord with the calculated depth of intrusion of the Rustenburg Layered Suite (Maier et al., 2016). We therefore propose that the key geochemical characteristics of the

Dullstroom rhyolite (and the entire Rooiberg Group) was imparted at this pressure (ca. 2.5 kbar) and depth, prior to eruption.

6.1 Fractional crystallisation (FC)

From the modeling results, the average low-Ti (LTI) magma and B1 were the only liquids that fractionated to produce a siliceous composition (Fig. 7). As fractionation progressed, the LTI melt produces a line of descent with greater initial Fe-enrichment and high concentrations of alkalis as Fe is depleted (Fig. 7). The low-Ti magma produced the most evolved composition of 73 wt.% SiO_2 at 961ºC, with clinopyroxene (11%), feldspar (54%) and quartz (31%) representing proportions of the crystallizing phases. Other minerals that crystallize in minor quantities include spinel and apatite. The most evolved products of the LTI fractionation are akin to the alkali contents of the upper Damwal, Kwaggasnek and Schrikkloof formations. Noteworthy is that the trend exhibited by the LTI does not intersect the Dullstroom rhyolite composition but plots closer to the boundary representing alkali (A) and iron (F) compositions (Fig.7a). On the other hand, the B2 and B3 modeled liquids generated liquid lines that show a maximum SiO_2 compositions of 68 wt.% and 69 wt.% respectively. These compositions are not as silicic (>70 wt.%) as is required for the Dullstroom rhyolites. In addition, the SiO_2 compositions of the modeled B2 and B3 liquids are representative of the most evolved products during fractionation at 1022ºC and 1018ºC, respectively. This implies that after complete fractionation, the B2 and B3 liquids cannot generate a composition that is high enough in SiO_2 to represent the Dullstroom and ferroan rhyolites ($SiO_2 \geq 70$ wt.%).

The only liquid whose evolution intersects the composition of Dullstroom rhyolites in Fig. 7a is B1, having its most evolved components with a composition of 69 wt.% SiO_2 at ~951ºC having undergone fractional crystallisation of orthopyroxene (50%), clinopyroxene (9%), feldspar (37 %) and quartz (3%) as crystallizing phases from the cooling liquid. The point at which the line representing fractionation of the B1 liquid intersects the Dullstroom rhyolite composition is observed at about 60% fractionation of the B1 liquid. Hence, modeling supports a view that the possible parental liquid to the Dullstroom rhyolites was similar to B1. The B1 melt shows a low initial Fe-enrichment whose composition also becomes alkali-rich as Fe is depleted during fractionation. However, it is also evident that at ~60% fractionation, the composition of the B1 liquid (Fig. 7a) intersecting the Dullstroom rhyolites has only 60 wt.% SiO_2 (Fig. 7c). This is less than that of the Dullstroom rhyolite which shows a SiO_2 concentration that is greater than 75 wt.% (>70% in other studies such as Schweitzer et al., 1995; Mathez et al., 2013). Furthermore, the fractionation trend of the B1 liquid as shown in Fig. 7c at ~60 % fractionation shows a much higher MgO (~4 wt.%) composition than those of the Dullstroom rhyolite. Therefore, the B1 liquid is unlikely to yield the Dullstroom rhyolite through fractionation alone.

6.2 Assimilation and fractional crystallisation (AFC)

After observing that fractionation alone cannot produce the Dullstroom rhyolite from the modeled parental compositions, assimilation of crustal material during fractional crystallisation was investigated (AFC) to test whether the combination of these processes could yield the Dullstroom rhyolite. Similar to Günther et al. (2018), several continental crustal compositions were used as the assimilant in modeling. James et al. (2001, 2003) and Nguuri et al. (2001) suggest that the thinnest crust in this region is ca. 35-40 km, reaching ~50 km below the BMP with lithospheric cratonic roots extending to about 250-300 km beneath the Kaapvaal Craton, therfore supporting the presence of a thick crust in the Bushveld Province which could have been incorporated during Bushveld magmatism. These authors suggested that the profile beneath the BMP consists of an upper crust and a lower crust that are felsic and intermediate in composition, respectively. The average compositions of granitoids and gneisses from the Johannesburg and Vredefort Dome (Buchanan et al., 2002; Günther et al., 2018; Lana et al. (2004)) representing country rocks were used to simulate upper crustal contaminating material, while the average amphibolite (mafic granulite and gneiss) and granulite (gneiss) were used to represent contamination from the lower crust. Noteworthy in this study is that we have excluded the Transvaal Supergroup as contaminants because these rocks typically overlie the Bushveld.

From the AFC model (Fig. 8), a B1 starting composition generated a Dullstroom rhyolite-like liquid composition (SiO_2 ≥70 wt.%) at ~1112ºC with ~30% of the melt fractionated (Fig. 8b). This liquid has 1.97 wt.% MgO and 70.04 wt.% SiO_2 and formed after having fractionally crystallised orthopyroxene (73%) and feldspar (27%). The AFC of B1 generates a composition akin to the rhyolites of the upper formations at ~1002ºC, after ~87% of fractionation of the B1 liquid (Fig. 8b) with 0.85 wt.% MgO and 70.37 wt.% SiO_2 , after having crystallized orthopyroxene (42%), clinopyroxene (7%), feldspar (36%) and quartz (14%). The temperature during the modeled fractionation implies that the magnesian Dullstroom rhyolite evolved at a higher temperature than the ferroan rhyolites of the upper Damwal, Kwaggasnek and Schrikkloof formations. In contrast, the AFC model assimilating ~15-20% lower crust produced the most evolved liquid with SiO_2 ~69 wt.% at 1009ºC after having crystallized olivine (23%), clinopyroxene (23%), feldspar (48%) and spinel (6%). The product of the AFC of lower crust produces a more mafic composition (leading to the fractionation of olivine) than the AFC models for the upper crust, as shown in Table 2. We therefore propose in our work that the most likely parental magma that evolved the Dullstroom rhyolite had a composition similar to the B1 liquid and further, that this liquid cannot have been the same as the magma that evolved the ferroan rhyolites of the Damwal, Kwaggasnek and Schrikkloof formations.

6.3 Parental magma of the Dullstroom rhyolite

Despite other authors (e.g., Buchanan et al., 1999; Günther et al. 2018) having modeled and proposed that the ferroan and intermediate to silicic lavas of the Rooiberg Group evolved from the magnesian lavas, this work shows that the modeled fractionation trend generated by crustal assimilation during crystallization of the LTI liquid does not simulate a composition equivalent to the Dullstroom rhyolite (Fig. 7). In addition, the end product of fractional crystallization as seen in the liquid lines of descent shows a higher alkali content than displayed by the Dullstroom rhyolite (Figs. 7 and 8). Hence, fractional crystallization, if responsible for the ferroan lavas, might not have occurred from a similar source to that which evolved the Dullstroom rhyolite. Therefore, if the Dullstroom rhyolite is more related to the other mafic lavas in the Dullstroom Formation and all are compositionally distinct to the ferroan lavas in the younger formations, it is unlikely that the ferroan lavas evolved from the mafic lavas, similar to the proposition by Twist (1985) and Twist and Harmer (1987).

Akin to Mathez et al. (2013) and Buchanan et al. (1999), the Dullstroom rhyolite has incompatible element concentrations such as V, Cr, Nb and Zr (Fig. 6) similar to the other magnesian lavas (mainly the LTI and HTI) of the Dullstroom Formation. The Dullstroom rhyolite composition is similar to continental volcanic rocks that are enriched in incompatible elements, either from partial melting of enriched mantle source areas or assimilation of continental crust (Thompson et al., 1983, 1984; Buchanan et al., 1999). This implies that the higher incompatible element contents of the Dullstroom rhyolite reflect evolution from either of these sources. Hence, a model of possible evolution of the Dullstroom rhyolites and the Rooiberg Group will be considered in future work.

Barnes et al. (2010) showed that the B1 magma exhibits incompatible element concentrations consistent with the composition of a primitive mantle melt (such as might have formed by contamination of a komatiitic basalt melt by upper continental crust) - a notion consistent with the Sr and O isotopic data of Maier et al. (2000) and Harris et al. (2005). We therefore propose, based on the similarities between the Dullstroom rhyolite and the B1 melt, that the former may have evolved from a composition (such as a basalt) similar to the latter. These characteristics further confirm that the Dullstroom rhyolite is not petrogenetically related to the ferroan lavas of the Damwal, Kwaggasnek and Schrikkloof formations. In addition, the Bushveld granite and granophyre are more similar to the ferroan lavas of the upper Rooiberg successions (as shown in Mathez et al., 2013) than they are the magnesian lavas of the Dullstroom Formation. Hence because the ferroan lavas are unrelated to the magnesian Dullstroom rhyolite, the granitic or granophyric components of the BMP be are also unlikely to be related to the Dullstroom rhyolite. Comparison between the Dullstroom rhyolite and other magnesian rhyolites around the world would be useful to fully understand the evolution of this distinct class of rhyolites.

7. Conclusion

Despite similar SiO_2 contents compared with the ferroan rhyolites in the Damwal, Kwaggaasnek and Schrikkloof formations, the Dullstroom rhyolite exhibits higher amounts of MgO and CaO. Trace element data suggest that the Dullstroom rhyolite evolved from a more mafic parental composition in comparison to the rhyolites of the overlying formations. MELTS modeling shows that the low-titanium basalt of the Dullstroom Formation could not have shared the same source as the Dullstroom rhyolite, nor could the proposed Bushveld source magmas B2 and B3 have led to their formation through fractional crystallisation. Instead, the modeling suggests that the Dullstroom rhyolite formed through assimilation of the upper crust (~20%) during fractionation of the B1 liquid that produced the Lower Zone and Lower Critical Zone of the Rustenburg Layered Suite. This would appear to be logical since it relates the earliest pulse of extrusive volcanism, at the base of the Rooiberg Formation, to the initial pulses of mafic intrusive activity in the basal portions of the RLS. However, it remains unclear as to why this early volcanism yielded a substantial volume of felsic melt, and where (if at all) the intrusive equivalent of this magma might be found. Further studies into the precise dating of each unit within the Rooiberg Group, and in particular the Dullstroom rhyolite, is therefore paramount in understanding its onset and duration of magmatism within the

Bushveld Magmatic Province. The occurrence of the Dullstroom rhyolite at the base of the Bushveld stratigraphy is interpreted as one of the first magmatic manifestations of the Bushveld LIP, although its confinement to the Dullstroom area southeast of the BMP also remains problematic.

Acknowledgments

L. Robb acknowledges thesupport of the DST-NRF Centre of Excellence for Integrated Mineral and Energy Resource Analysis (DST-NRF CIMERA) towards this research. Opinions expressed and conclusions arrived at, are those of the authors and are not necessarily attributed to the CoE. N. Lenhardt thanks the National Research Foundation of South Africa (NRF) (grant no. 90800) and the University of Pretoria for their financial support. We thank Jeanette Dykstra for the XRF analyses used in this project and Grant Bybee for his invaluable guidance during MELTS modeling. E.A. Mathez is thanked for his invaluable comments on an early version of the manuscript. We thank an anonymous reviewer for the comments on this manuscript and Mohamed G. Abdelsalam for his editorial handling.

References

Barnes, S.-J., Maier, W. D., Curl, W. A., 2010. Composition of the marginal rocks and sills of the Rustenburg Layered Suite, Bushveld Complex, South Africa: implications for the formation of the platinum-group element deposits. Econ. Geol. 105, 1491–1511.

Borrok, D.M., Kelser, S.E., Boer, R.H. and Essene, E.J., 1998. The Vergenoeg magnetite-fluorite deposit, South Africa; support for a hydrothermal model for massive iron oxide deposits. Economic Geology, 93(5), 564-586.

Branney, M.J., Bonnichsen, B., Andrews, G.D.M., Ellis, B., Barry, T.L. and McCurry, M., 2008. 'Snake River (SR)-type'volcanism at the Yellowstone hotspot track: distinctive products from unusual, high-temperature silicic super-eruptions. Bulletin of Volcanology, 70(3), 293-314.

Bryan, S.E., Riley, T.R., Jerram, D.A., Leat, P.T., Stephens, C.J., 2002. Silicic volcanism: an under-valued component of large igneous provinces and volcanic rifted margins. In: Menzies, M.A., Klemperer, S.L., Ebinger, C.J., Baker, J. (Eds.), Magmatic Rifted Margins. Geological Society of America Special Paper, 362, pp. 99–120.

Buchanan, P.C., Koeberl, C., Reimold,W.U., 1999. Petrogenesis of the Dullstroom Formation, Bushveld Magmatic Province, South Africa. Contributions to Mineralogy and Petrology, volume 137, 133-146.w

Buchanan, P.C., Reimold, W.U., Koeberl, C., Kruger, F.J., 2002. Geochemistry of intermediate to siliceous volcanic rocks of the Rooiberg Group, Bushveld Magmatic

Province, South Africa. Contributions to Mineralogy and Petrology, volume 144, 131-143.

Buchanan, P.C., Reimold, W.U., Koeberl, C., Kruger, F.J., 2004. Rb–Sr and Sm–Nd iso-topic compositions of the Rooiberg Group, South Africa: early Bushveld-related volcanism. Lithos volume 29, 373–388.

Cheney, E.S., Twist, D., 1991. The comformable emplacement of the Bushveld mafic rocks along a regional uncomformity in the Transvaal succession of South Africa. Precambrian Research, volume 52, 115-132.

Coertze, F.J., Burger, A.J., Walraven, F., Marlow, A.G., MacCaskie, D.R., 1978. Fieldrelations and age determinations in the Bushveld Complex. Trans. Geol. Soc. S. Afr. 81, 1-11.

Eriksson, P.G., Hattingh, P.J., Altermann, W., 1995. An overview of the geology of theTransvaal Sequence and Bushveld Complex, South Africa. Miner. Depos. 30,98-111.

Eriksson, P.G., Schreiber, U.M., Reczko, B.F.F., Snyman, C.P., 1994. Petrography and geochemistry of sandstones interbedded with the Rooiberg Felsite Group (Transvaal Sequence, South Africa): implications for provenance and tectonic setting. J. Sediment. Res., Sect. A Sediment. Pet. Proc. 64, 836– 846.

Ernst, R.E., Buchan, K.L., 2001. Large mafic magmatic events through time and links to mantle plume-heads, in: Ernst, R.E., Buchan, K.L. (Eds.), Mantle Plumes: Their identification through time. Geol. Soc. Am. Spec. Pap. 352, 483-575.

Fernandes, C.M.D., Juliani, C., Monteiro, L.V.S., Lagler, B. and Misas, C.M.E., 2011. High-K calc-alkaline to A-type fissure-controlled volcano-plutonism of the São Félix do Xingu region, Amazonian craton, Brazil: Exclusively crustal sources or only mixed Nd model ages? Journal of South American Earth Sciences, 32(4), 351-368.

Frost, B.R., Barnes, C.G., Collins, W.J., Arculus, R.J., Ellis, D.J., Frost, C.D., 2001. A geochemical classification for granitic rocks. J. Petrol., 42(11), 2033-2048.

Frost, C.D., Frost, B.R., 2011. On ferroan (A-type) granitoids: their compositional variability and modes of origin. J. Petrol. 52(1), 39-53.

Ghiorso, M.S., Gualda, G.A.R., 2015. An H_2O–CO_2 mixed fluid saturation model compatible with rhyolite-MELTS. Contrib Miner Petrol 169(6), 1-30.

Günther, T., Haase, K. M., Klemd, R., & Teschner, C., 2018. Mantle sources and magma evolution of the Rooiberg lavas, Bushveld Large Igneous Province, South Africa. Contributions to Mineralogy and Petrology, 173(6), 51.

Harmer, R.E., Armstrong, R.A., 2000. New precise dates on the acid phase of the Bushveld and their implications. Abstract. Workshop on the Bushveld Complex, 18th-21st November 2000, Burgersfort. University of Witwatersrand, Johannesburg.

Harmer, R.E., Sharpe, M.R., 1985. Field relations and strontium isotope systematics of the marginal rocks of the eastern Bushveld Complex. Econ. Geol. 80(4), 813-837.

Harris, C., Pronost, J.J., Ashwal, L.D., Cawthorn, R.G., 2005. Oxygen and hydrogen isotope stratigraphy of the Rustenburg Layered Suite, Bushveld Complex: constraints on crustal contamination. J. Petrol. 46(3), 579-601.

Hartzer, F.J., 1995. Transvaal Supergroup inliers: geology, tectonic development and relationship with the Bushveld Complex, South Africa. J. Afr. Earth Sci. 21(4), 521-547.

Hatton, C.J., Schweitzer, J.K., 1995. Evidence for synchronous extrusive and intrusiveBushveld magmatism. J. Afr. Earth Sci. 21, 579-594.

Irvine, T.N., Baragar, W.R.A., 1971. A guide to the chemical classification of the common rocks. Can J Earth Sci 8, 523-548.

James, D.E., M.J. Fouch, J.C. VanDecar, S. van der Lee, Kaapvaal Seismic Group, 2001. Tectospheric structure beneath southern Africa. Geophys. Res. Lett. 28, 2485-2488.

James, D.E., Niu, F., Rokosky, J., 2003. Crustal structure of the Kaapvaal craton and its significance for early crustal evolution. Lithos71(2):413–429.

Jolayemi, O.O., 2015. Chemical Evolution of the Paleoproterozoic Rooiberg Group, Kaapvaal Craton, South Africa: New Insights into the Formation of a Silicic Large Igneous Province (SLIP). PhD thesis. University of Pretoria.

Kinnaird, J.A., 2005. The Bushveld large igneous province. Review Paper. The University of the Witwatersrand, Johannesburg, 39.

Kruger, F.J., 2005. Filling the Bushveld Complex magma chamber: lateral expansion, roof and floor interaction, magmatic unconformities, and the formation of giant chromitite, PGE and Ti‑V-magnetitite deposits. Miner. Depos. 40, 451–472.

Lana, C., Reimold, W.U., Gibson R.L., Koeberl, C., Siegesmund, S., 2004. Nature of the Archeanmidcrust in the core of the VredefortDome, central Kaapvaal Craton, South Africa. Geochim Cosmochim Acta 68 (3), 623-642.

Lenhardt, N., Eriksson, P.G., 2012. Volcanism of the Paleoproterozioc Bushveld Large Igneous Province: The Rooiberg Group, Kaapvaal Craton, South Africa. Precambrian Research volume 214-215, 82-94.

Lenhardt, N., Masango, S.M., Jolayemi, O.O., Lenhardt, S.Z., Peeters, G.-J., Eriksson, P.G., 2017. The Palaeoproterozoic (~2.06 Ga) Rooiberg Group, South Africa:

Dominated by high-grade lava-like and rheomorphic ignimbrites? New observations and lithofacies analysis. Journal of African Earth Sciences, 131, 213-232.

Maier, W.D., Arndt, N.T., Curl, E.A., 2000. Progressive crustal contamination of the Bushveld Complex: evidence from Nd isotopic analyses of the cumulate rocks. Contrib Mineral Petrol 140, 316-327.

Maier, W.D., Barnes, S.J., Karykowski, B.T., 2016. A chilled margin ofkomatiite and Mg-rich basaltic andesite in the western Bushveld Complex, South Africa. Contrib Miner Petrol 171(6):1–22.

Maier, W.D., Prevec, S.A., Scoates, J.S., Wall, C.J., Barnes, S.J., Gomwe, T., 2018. The Uitkomst intrusion and Nkomati Ni-Cu-Cr-PGE deposit, South Africa: trace element geochemistry, Nd isotopes and high-precision geochronology. Mineralium Deposita, 53(1), 67-88.

Manley, C.R., 1996. In situ formation of welded tuff-like textures in the carapace of a voluminous silicic lava flow, Owyhee County, SW Idaho. Bulletin of volcanology, 57(8), 672-686.

Mapeo, R.B.M., Ramokate, L.V., Corfu, F., Davis, D.W., Kampunzu, A.B., 2006. The Okwa basement complex, western Botswana: U-Pb zircon geochronology and implications for Eburnean processes in southern Africa. J. Afr. Earth Sci. 46, 253-262.

Mathez, E.A., VanTongeren, J.A., Schweitzer, J., 2013. On the relationships between the Bushveld Complex and its felsic roof rocks, part 1: petrogenesis of Rooiberg and related fesites. Contributions to Mineralogy and Petrology, volume 166, 435-449.

Moore, I., Kokelaar, P., 1998. Tectonically controlled piecemeal caldera collapse: A case study of Glencoe volcano, Scotland. Geological Society of America Bulletin, 110(11), 1448-1466.

Nesbitt, H.W., Young, G.M., 1982. Early Proterozoic climates and plate motions inferred from major element chemistry of lutites. Nature, volume299, 715-717.

Nguuri, T.K., Gore, J., James, D.E., Webb, S.J., Wright, C., Zengeni, T.G., Gwavava, O., Snoke, J.A., Kaapvaal Seismic Group, 2001. Crustal structure beneath southern Africa and its implications for the formation and evolution of the Kaapvaal and Zimbabwe cratons. Geophysical Research Letters 28, 2501-2504.

Reichardt, F.J., 1994. The Molopo Farms Complex, Botswana: History, stratigraphy, petrography, petrochemistry and Ni-Cu-PGE mineralization. Explor. Min. Geol. 3, 263-284.

Rudnick, R.L. and Gao, S., 2003. Composition of the continental crust. The crust, 3, 1-64.

Schweitzer, J.K., Hatton, C.J., de Waal, S.A., 1995. Regional lithochemical stratigraphy of the Rooiberg Group, upper Transvaal Supergroup: A proposed new subdivision. South African Journal of Geology, volume 98, 245-255.

Scoates, J.S. and Friedman, R.M., 2008. Precise age of the platiniferous Merensky Reef, Bushveld Complex, South Africa, by the U-Pb zircon chemical abrasion ID-TIMS technique. Economic Geology, 103(3), pp.465-471.

Scoates, J.S., Wall, C.J., 2015. Geochronology of layered intrusions. In Layered intrusions (3-74). Springer, Dordrecht.

Thompson, R.N., Morrison, M.A., Dickin, A.P., Hendry, G.L., 1983. Continental food basalts. arachnids rule OK? In: Hawkesworth CJ, Norry MJ (eds.) Continental basalts and mantle xenoliths. Shiva Publishing, Nantwich, 158-185.

Thompson, R.N., Morrison, M.A., Hendry, G.L., Parry, S.J., Simpson, P.R., Hutchison, R., O'Hara, M. J., 1984. An assessment of the relative roles of crust and mantle in magma genesis: an elemental approach. Philosophical Transaction Royal Society of London A310, 549-590.

Twist, D., French, B.M., 1983. Voluminous acid volcanism in the Bushveld Complex: a review of the Rooiberg Felsite. Bulletine volcanologique, volume 46(3), 225-242.

Twist, D., 1985. Geochemical evolution of the Rooiberg Silicc Lavas in the Loskop Dam Area, Southeastern Bushveld. Economic Geology, volume 80, 1153-1165.

VanTongeren, J.A., Mathez, E.A., Kelemen, P.B., 2010. A felsic end to Bushveld differenciation. Journal of Petrology, volume 51, 1891-1912.

Von Gruenewaldt, G., 1968. The Rooiberg felsite north of Middelburg and its relation to the layered sequence of the Bushveld Complex. South African Journal of Geology, 71(2), 153-172.

Walraven, F., 1982. Textural, geochemical and genetical aspects of the granophyric rocks of the Bushveld Complex: Unpub (Doctoral dissertation, Ph. D. thesis, Univ. Witswatersrand).

Walraven, F., 1997. Geochronology of the Rooiberg Group, Transvaal Supergroup, South Africa. Information circular, Economic Research Unit, University of Witwatersrand, Johannesburg, South Africa, volume 97, 316.

Walraven, F. and Hattingh, E., 1993. Geochronology of the Nebo Granite, Bushveld Complex. S. Afr. J. Geol. 96, 31-41.

White, J.D.L., Bryan, S.E., Ross, P.-S., Self, S., Thordarson, T., 2009. Physical volcanology of continental large igneous provinces: update and review. Special Publication IAVCEI, 2. 291–321.

Wilson, J., Ferre, E.C., Lespinasse, P., 2000. Repeated tabular injection of high-level alkaline granites in the eastern Bushveld, South Africa. J Geol Soc Lond 157(5):1077-1088.

Worst, B.G., 1944. Die geologie noord van Loskopdam, bosveldse kompleks (Doctoral dissertation, Universiteit van Pretoria.).

Zeh, A., Ovtcharova, M., Wilson, A.H., Schaltegger, U., 2015. The Bushveld Complex was emplaced and cooled in less than one million years – results of zirconology, and geotectonic implications. Earth Planet. Sci. Lett. 418, 103-114.

Figure captions:

Figure 1. Geological map of the Bushveld Magmatic Province, including the Rustenburg Layered Suite, the Rooiberg Group, the Rashoop Granophyre Suite and the Lebowa Granite Suite (modified after Hartzer, 1995, and Kruger, 2005). The inset shows the location of the area in South Africa. The red rectangle represents the study area near Dullstroom, Mpumalanga Province.

Figure 2. General schematic representation highlightingthe lithologies of the Rooiberg Group and their relationship with other rocks within the Bushveld Magmatic Province (modified after SACS, 1980; Walraven, 1982; Harmer and Sharpe, 1985, and Schweitzer et al., 1995). Details are explained in Lenhardt et al. (2017). The term rhyolite is used in this graphic to highlight previous literature subdivisions.

Figure 3. General lithostratigraphy of the Dullstroom Formation showing the major lithologies exhibited in the study area near Dullstroom.

Figure 4. Examples for the Rooiberg Group rhyolites. (a) Dullstroom Formation rhyolite; b) Damwal Formation rhyolite; c) Kwaggasnek Formation rhyolite; d) Schrikkloof Formation rhyolite. Samples b-d were interpreted as ignimbrites that underwent high to very high degrees of welding (see Lenhardt et al., 2017 for details).

Figure 5. Geochemical comparison of the rhyolites of the Rooiberg Group. (a) modifiedalkali-lime index (MALI = wt.% Na_2O + K_2O - CaO) against SiO_2; (b) Fe-index = wt% $FeO_T/(FeO_T + MgO)$ versus SiO_2; (c) aluminum saturation index [ASI = at.% Al/(Ca -1.67P + Na + K)]. All fields are after Frost and Frost (2001).

Figure 6. Comparison of the average trace element concentration between the Dullstroom rhyolite and the rhyolites of the Damwal, Kwaggasnek and Schrikkloof formations. All rhyolite compositions are normalised to bulk continental compositions of Rudnick and Gao (2003).

Figure 7. MELTS modeling of the possible sources of the rhyolitic compositions within the Rooiberg Group using Rhyolite-MELTS (Ghiorso and Gualda, 2015) and comparison with the actual compositions. Average low-Ti and B1compositions are modeled and investigated as possible sources for the Dullstroom rhyolite: (a) AFM MELTS model fractionation trends and results; (b) actual AFM composition plots across the Rooiberg stratigraphy; (c) Results of MELTS modeled fractionation trend as displayed by the SiO_2 vs MgO plot; (d) actual plot of the SiO_2 vs MgO composition across the Rooiberg stratigraphy. Dark dots in (a) and (c) represent the Dullstroom rhyolite. The dashed lines in (a) and (b) represent the boundaries (according to Irvine and Barragar, 1971) between the calc-alkaline and tholeiitic series.

Figure 8. Model results showing the comparison between the fractionation of the B1 liquid and the fractionation and assimilation of the same liquid using Rhyolite-MELTS

(Ghiorso and Gualda, 2015): (a) AFM model results comparing assimilation and fractional crystallisation with the singular process of crystallisation of the B1 liquid; (b) SiO_2 vs MgO plot of the comparison between the model results of assimilation and fractional crystallisation with the singular process of crystallisation of the B1 liquid.

Table captions:

Table 1. Selected major element oxides and selected trace element data of the Rooiberg Group samples.The complete data set can be found in Jolayemi (2015).

Table 2. Details showing the MELTS parameters used in modeling the evolution of the Dullstroom rhyolites.

Table 3: Compositions generated from the MELTS modeling program and comparison of the Dullstroom rhyolite with the compositions from the LTI, B1, and B1 with assimilation (ass.). ADR- is the average composition of the Dullstroom rhyolites.

Sample name	Latitude	Longitude	Formation	SiO_2 (wt.%)	TiO_2 (wt.%)	Al_2O_3 (wt.%)	Fe_2O_3 (total) (wt.%)	MnO (wt.%)	MgO (wt.%)	CaO (wt.%)	Na_2O (wt.%)	K_2O (wt.%)	P_2O_5 (wt.%)	Cr_2O_3 (wt.%)	NiO (wt.%)	V_2O_5 (wt.%)	ZrO_2 (wt.%)	LOI	CIA	Y (ppm)	Zr (ppm)	Nb (ppm)	Rb (ppm)	Ba (ppm)	Sr (ppm)	V (ppm)	Cr (ppm)	Th (ppm)
SM-25	S 25°25'16,1"	E 29°31'37,5"	Schrikkloof	73.93	0.25	11.73	3.5	0.06	0.05	0	3.24	4.52	0.01	0.01	0.01	0	0.06	1.58	60.18	74.2	312	23.1	158	877	54.5	1.15	1.38	26.1
SM-28.2	S 25°25'07,0"	E 29°31'32,1"	Schrikkloof	74.28	0.29	12.13	3.94	0.08	0.3	0	3.39	4.54	0.02	0.01	0	0	0.06	1.08	60.47	87.2	328	24.2	158	963	61.9	1.54	2.78	24.7
SM-5.2	S 25°24'12,4"	E 29°30'12,0"	Schrikkloof	73.47	0.21	12.9	3.48	0.02	0.03	0	2.99	5.35	0.03	0	0	0	0.03	1.57	60.73	34.9	226	20.8	184	571	101	8.91	3.4	35.1
SM-18.1	S 25°26'00,0"	E 29°31'44,8"	Schrikkloof	76.37	0.24	10.92	3.37	0.04	0.04	0.12	2.33	5.19	0.01	0	0	0	0.06	0.86	58.84	71	427	20.1	184	1149	68.6	0.19	0.61	23.4
SM-19	S 25°25'59,3"	E 29°31'43,8"	Schrikkloof	73.72	0.27	12.08	3.7	0.03	0.02	0.06	2.54	5.73	0.01	0	0	0	0.06	1.21	59.89	62.2	480	23.7	207	1269	82.7	0.62	0.93	25.6
SM-22	S 25°25'19,7"	E 29°31'39,8"	Schrikkloof	79.54	0.26	7.7	4.38	0.07	0.08	0.74	1.98	2.97	0.05	0.02	0.01	0	0.04	1.31	57.51	46.2	268	13.5	103	679	53	0.58	2.38	15
SM-48	S 25°24'14,6"	E 29°30'42,3"	Kwaggasnek	70.11	0.41	11.59	6.78	0.14	0.12	1.04	2.47	4.58	0.05	0.01	0.01	0	0.05	1.91	58.89	57.7	368	18	154	971	80.7	0.3	0.7	21.7
SM-4.1	S 25°24'13,1"	E 29°30'06,7"	Kwaggasnek	80.84	0.4	7.13	5.35	0.05	0.13	0	0.01	3.61	0.07	0.01	0	0.01	0.03	1.94	66.32	12.6	170	5.38	140	900	57.7	29.1	57.9	9.68
LD016	S 25°25'09,8"	E 29°22'04,6"	Kwaggasnek	69.44	0.37	11.12	5.64	0.09	<0.01	2.07	1.96	5	0.03	<0.01	<0.01	<0.01	0.05	2.97	55.19	60.7	352	16.5	189	1953	69	0.28	0.17	21.5
LD07	S 25°25'11,9"	E 29°22'59,1"	Kwaggasnek	69.86	0.4	12.4	6.61	0.06	0.07	0.59	2	4.01	0.08	0.01	<0.01	<0.01	0.06	2.46	65.26	67.6	372	18	147	1197	62	0.75	1.77	21
LD018	S 25°25'06,0"	E 29°22'01,0"	Kwaggasnek	70.74	0.41	11.75	6.57	0.09	0.06	0.14	2.58	4.22	0.04	<0.01	<0.01	<0.01	0.05	1.85	62.87	60.3	369	17.2	134	1197	32.2	0.24	0.72	20.6
LD04	S 25°25'14,0"	E 29°22'59,9"	Kwaggasnek	74.19	0.39	12.21	5.75	0.03	0.04	<0.01	1.54	5.24	0.03	<0.01	<0.01	<0.01	0.04	1.85	na	42.6	373	17.2	192	861	16	1.1	0.38	21.5
LD02	S 25°25'16,6"	E 29°22'59,9"	Kwaggasnek	71.24	0.37	11.32	7.37	0.12	<0.01	<0.01	2.76	4.1	0.03	<0.01	<0.01	<0.01	0.05	1.61	na	55.3	360	16.9	147	811	28.1	0.84	1.35	22.6
LD015	S 25°25'12,3"	E 29°22'04,1"	Kwaggasnek	77.08	0.36	11.41	1.49	<0.01	<0.01	<0.01	1.68	5.3	0.02	<0.01	<0.01	<0.01	0.05	1.55	na	50.9	347	15.8	172	639	19.7	1.7	0.28	20.1
LD012A	S 25°25'12,6"	E 29°22'19,3"	Kwaggasnek	69.8	0.38	11.47	5.94	0.11	0.1	2.49	1.23	5.1	0.03	<0.01	<0.01	<0.01	0.04	4.93	56.53	54.2	354	17	199	724	48.2	0.38	0.37	21.9
LD012B	S 25°25'12,6"	E 29°22'19,3"	Kwaggasnek	68.94	0.37	11.14	5.76	0.13	0.02	2.08	1.83	5.07	0.03	0.01	<0.01	<0.01	0.05	3.05	56.37	62	348	16.7	201	2077	69.4	0.31	0.24	21.6
LD09	S 25°25'14,2"	E 29°22'28,5"	Kwaggasnek	69.34	0.39	12.58	6.15	0.1	0.05	2.01	2.4	5.05	0.03	<0.01	<0.01	<0.01	0.04	3.06	na	56.3	349	16.5	175	1158	65.5	0.24	0.25	21.7
LD017	S 25°25'08,4"	E 29°22'02,7"	Kwaggasnek	70.88	0.39	13.21	5.18	0.01	0.1	<0.01	2.99	4.69	0.05	<0.01	<0.01	<0.01	0.05	1.9	na	46	352	16.4	140	978	30.8	0.45	0.42	17.1
LD08	S 25°25'15,7"	E 29°22'28,6"	Kwaggasnek	76.18	0.37	13.28	1.11	0.01	0.01	<0.01	0.42	6.21	0.02	<0.01	<0.01	<0.01	0.05	1.91	na	54.6	358	16.3	212	2370	23.3	1.03	1.44	21.5
LD010	S 25°25'13,1"	E 29°22'29,1"	Kwaggasnek	71.91	0.39	11.79	5.96	0.04	0.02	<0.01	1.57	4.81	0.06	<0.01	<0.01	<0.01	0.06	2.04	na	63.9	378	17.6	175	1054	25	0.76	0.71	21.6
LD011	S 25°25'12,3"	E 29°22'29,8"	Kwaggasnek	71.97	0.42	11.26	6.17	0.03	<0.01	<0.01	2.38	4.9	0.03	<0.01	<0.01	<0.01	0.05	1.48	na	57.2	378	18.4	171	875	30.2	0.48	0.65	21.3
LD013	S 25°25'10,7"	E 29°22'19,4"	Kwaggasnek	73.81	0.39	11.27	3.65	0.05	<0.01	1.56	2.41	4.31	0.04	<0.01	<0.01	<0.01	0.05	2.33	57.65	60.1	343	15.3	164	728	54.6	0.27	0.66	20
SM-23	S 25°25'17,5"	E 29°31'38,4"	Damwal	69.11	0.58	11.62	7.14	0.14	0.26	2.62	2.23	4.6	0.12	0.01	0	0	0.04	1.6	55.15	49.5	313	16.2	132	869	114	1.77	0.57	18.5
SM-38.1	S 25°24'10,7"	E 29°30'27,8"	Damwal	70.12	0.56	11.43	7.33	0.07	0.07	3.63	3.34	1.23	0.13	0	0.01	0	0.04	1.81	58.23	40.4	269	13.8	54.2	198	353	15.1	2.53	15.8
SM-44.1	S 25°24'14,7"	E 29°30'28,7"	Damwal	67.08	0.66	12.04	7.8	0.14	0.68	2.1	3.59	3.05	0.17	0	0	0.01	0.04	1.73	57.94	39.6	290	14.3	91	737	125	20.4	0.96	18.2
SM-45.1	S 25°24'13,8"	E 29°30'31,5"	Damwal	68.27	0.65	12.38	7.52	0.11	0.4	2.56	3.59	3.47	0.17	0	0	0	0.04	1.65	56.27	41.6	287	14.4	103	512	253	14.4	2.57	18.1
SM-50	S 25°24'13,7"	E 29°30'48,4	Damwal	69.06	0.53	11.83	7.39	0.12	0.17	1.19	2.74	4.97	0.11	0	0	0	0.04	1.8	57.07	44.9	323	16	167	985	105	2.12	0.54	21.2
SM-51.1	S 25°24'12,0"	E 29°30'53,0"	Damwal	69.67	0.57	12.09	7.37	0.13	0.19	0.89	2.95	4.69	0.12	0	0	0	0.04	1.75	58.63	45.6	316	15.8	146	997	104	2.42	0.64	20.5
SM-RL1	S 25°23'44,0"	E 29°30'30,5"	Damwal	68.78	0.64	12.17	8.26	0.1	0.32	0.09	2.92	3.69	0.13	0	0	0	0.04	2.39	64.49	45.4	328	15.9	116	814	60.3	7.09	1.06	19.5
SM-3	S 25°24'13,1"	E 29°30'06,7"	Damwal	67.4	0.69	12.94	7.94	0.12	0.48	2.18	2.54	5.31	0.17	0	0	0	0.04	0.84	56.33	44.8	322	16.4	144	1216	138	13.7	1.64	19.9

SM-5.1	S 25°24'12,4"	E 29°30'12,0"	Damwal	66.07	0.65	11.94	9.77	0.16	0.44	2.55	2.82	3.75	0.23	0	0	0	0.04	1.29	56.7	51	296	16.5	122	852	154	2.18	0.92	16.7
SM-6	S 25°24'13,0"	E 29°30'13,9"	Damwal	67.63	0.6	12.03	9.03	0.13	0.32	1.74	2.92	4.16	0.17	0	0	0	0.04	1.08	57.7	53.2	319	17	145	136	897	1.7	0.39	17.8
SM-10	S 25°24'20,7"	E 29°30'25,6"	Damwal	71.89	0.44	11.4	5.85	0.06	0.11	0.91	2.33	4.99	0.07	0	0	0	0.05	1.81	58.07	69	355	18.2	186	997	90.5	0.38	0.75	20.3
SM-13	S 25°24'50,8"	E 29°30'37,1"	Damwal	72.86	0.64	11.22	6.21	0.12	0.91	0.59	2.44	2.73	0.13	0.02	0.01	0.01	0.06	1.86	66.08	32.1	385	12.9	107	1063	110	46.2	60.7	22.7
SM-14	S 25°24'48,8"	E 29°30'39,0"	Damwal	66.96	0.61	11.96	9.1	0.14	0.33	1.91	2.93	4.08	0.18	0	0	0	0.04	1.66	59.69	52.7	341	17.5	180	1088	116	3.65	4.43	20.5
LD028	S 25°25'07,9"	E 29°22'19,9"	Damwal	68.93	0.59	11.83	7.74	0.1	0.57	1.02	2.44	4.12	0.15	<0.01	<0.01	<0.01	0.03	2.13	60.95	41.1	282	13.1	126	1016	103	9.67	13.8	17.5
LD026	S 25°25'08,2"	E 29°22'44,7"	Damwal	65.65	0.5	11.42	8.05	0.12	0.25	2.8	1.86	4.56	0.1	<0.01	<0.01	<0.01	0.04	3.43	55.33	52.1	307	14.9	162	1006	111	0.88	0.27	19
LD019	S 25°25'02,1"	E 29°22'03,1"	Damwal	69.03	0.66	12.2	9.98	0.06	0.03	0.63	2.5	5.04	0.21	<0.01	<0.01	<0.01	0.04	1.34	59.89	43	288	14.6	172	1353	57.5	3.02	0.96	16.7
LD014	S 25°25'00,6"	E 29°22'21,9"	Damwal	67.19	0.64	11.77	9.87	0.06	0.03	0.61	2.41	4.93	0.21	<0.01	<0.01	<0.01	0.04	2.06	59.69	41.7	276	12.3	137	1289	124	24.1	14.3	13.2
LD020	S 25°24'58,4"	E 29°22'05,8"	Damwal	68.64	0.56	11.59	7.77	0.11	0.25	1.71	1.99	4.13	0.16	<0.01	<0.01	<0.01	0.04	3.02	59.68	39.5	272	12.6	158	651	51.2	10.6	12.2	16.4
LD021	S 25°24'55,1"	E 29°22'09,4"	Damwal	68.27	0.61	11.74	7.25	0.13	0.49	1.74	2.03	4	0.18	<0.01	<0.01	0.01	0.04	3.13	60.17	45.8	269	12.4	138	1798	88.3	9.98	11	15.8
RG7	S 25° 23' 02,0"	E 29° 58' 54,2"	Dullstroom	67.02	0.61	13.47	6.34	0.09	1.83	4.01	3.04	2.76	0.13	0.02	<0.01	0.02	0.03	1.18	58.08	21,95	190,81	8,29	66,77	529,34	253,09	107.98	121.65	3
RG8	S 25° 23' 02,7"	E 29° 58' 53,4"	Dullstroom	56.15	0.63	14.87	9.78	0.14	5.24	8.16	2.3	1.44	0.11	0.04	0.02	0.03	0.01	1.89	58.7	17,18	115,04	5,59	58,76	268,96	241,37	181.63	230.29	3
RG10	S 25° 23' 00,9"	E 29° 58' 48,4"	Dullstroom	53.97	1.42	11.29	11.81	0.25	5.66	8.44	2.77	1.9	0.14	0.07	0.03	0.04	0.02	0.97	46.27	18,77	178,62	7,21	84,67	558,92	249,05	109.58	117.06	3
RG13	S 25° 22' 56,3"	E 29° 58' 52,1"	Dullstroom	64.27	0.64	13.3	6.98	0.12	1.8	4.2	2.9	2.55	0.12	0.02	<0.01	0.02	0.03	1.79	52.44	20,41	197,06	7,27	64,39	516,15	209,55	111.91	131.4	4.49
RG21	S 25° 22' 29,1"	E 30° 00' 14,8"	Dullstroom	70.73	0.34	11.45	4.33	0.11	1.87	3.09	0.91	4.06	0.09	0.03	0.01	0.01	0.03	1.16	58.7	na	na	na	na	na	na	na	na	na
RG23	S 25° 22' 23,7"	E 30° 00' 03,7"	Dullstroom	75.26	0.29	11.22	3.94	0.08	1.41	2.53	0.98	4.34	0.07	0.02	0.01	0.01	0.03	1.05	58.81	9,72	171,87	4,43	126,46	903,42	183,05	53.21	130.09	3
RG24	S 25° 22' 28,1"	E 29° 59' 53,7"	Dullstroom	55.97	0.61	14.99	9.07	0.18	5.06	9.26	2.3	0.9	0.12	0.02	0.01	0.03	0.02	1.05	56.04	17,92	118,33	5,55	32,06	217,59	258,52	176.81	121.48	3
RG25	S 25° 22' 28,1"	E 29° 59' 53,7"	Dullstroom	57.99	1.62	13.32	11.28	0.15	3.86	7.54	2.53	1.35	0.17	0.02	0.01	0.04	0.02	1.16	55.91	27,31	189,49	13,57	55,67	254,81	375,25	215.34	69.51	3
RG34	S 25° 23' 42,9"	E 29° 56' 58,0"	Dullstroom	68.81	0.5	12.71	5.13	0.08	1.52	3.95	1.81	3.4	0.11	0.07	0.01	0.02	0.03	1.58	57.47	15,14	178,38	6,7	110,88	694,71	219,08	91.87	422.79	3
RG40	S 25° 23' 37,3"	E 29° 59' 57,8"	Dullstroom	61.66	0.71	14.52	9.74	0.16	3	6.3	2.6	1.73	0.17	0.02	0.01	0.03	0.02	1.18	54.61	25,82	172,06	7,34	57,69	426,85	232,41	178.39	90.72	3.05
RG41	S 25° 23' 44,4"	E 30° 00' 17,2"	Dullstroom	57.92	0.64	14.2	10	0.19	3.96	6.89	2.75	1.55	0.15	0.02	0.01	0.03	0.02	1.55	57.75	20,38	133,8	6,05	51,92	423,94	246,1	186.05	75.7	3
RG42	S 25° 23' 45,4"	E 30° 00' 16,3"	Dullstroom	42.25	0.46	11.08	7.82	0.15	3.69	6.58	1.37	0.8	0.09	0.01	0.01	0.02	0.01	25.67	57.85	18,09	118,53	6,41	53,86	320,8	238,17	183.65	118.88	3
RG45	S 25° 23' 50,0"	E 30° 00' 30,0"	Dullstroom	80.14	0.31	12.22	3.72	0.06	1.76	1.96	1.79	4.14	0.08	0.02	0.01	0.01	0.02	0.78	na	12,7	174,55	4,53	87,85	1534,07	185,65	54.21	135.71	3
RG47	S 25° 24' 01,7"	E 30° 00' 38,8"	Dullstroom	72.63	0.31	10.92	3.86	0.06	1.69	2.52	1.33	3.99	0.08	0.03	0.01	0.01	0.03	1.15	54.67	12,7	174,55	4,53	87,85	1534,07	185,65	54.21	135.71	3
RG49	S 25° 24' 10,2"	E 30° 00' 41,0"	Dullstroom	53.9	0.59	15.02	9.47	0.14	5.6	9.16	1.86	1.47	0.11	0.02	0.01	0.03	0.01	2.48	55.53	15,73	107,07	4,37	65,91	263,35	213,97	187.87	121.44	3
RG50	S 25° 24' 13,9"	E 30° 00' 43,8"	Dullstroom	59.05	0.41	13.28	9.84	0.19	4.23	8.72	2.77	0.56	0.06	0.03	0.01	0.03	0.01	0.99	55.86	13,95	97,04	5,83	24,85	194,05	249,01	175.91	222.32	3
RG51	S 25° 24' 15.9"	E 30° 00' 48,9"	Dullstroom	57.73	0.46	14.37	9.61	0.17	5.88	8.41	1.8	1.25	0.07	0.04	0.02	0.03	0.01	2.08	53.86	12,49	79,51	4,74	60,53	264,42	224,23	179.08	293.61	3
RG52	S 25° 24' 16.4"	E 30° 00' 46,0"	Dullstroom	55.57	0.45	14.05	9.52	0.16	6.17	8.51	1.93	1.25	0.06	0.04	0.02	0.03	0.01	1.89	58.53	12,68	79,04	5,85	64,64	187,98	225,33	188.38	323.01	3
RG54	S 25° 23' 57.9"	E 30° 00' 23,8"	Dullstroom	56.62	0.58	14.46	9.91	0.18	4.73	8.68	1.8	1.31	0.13	0.03	0.02	0.03	0.02	1.05	54.62	16,11	124,85	7,3	67,04	228,93	228,99	169.34	155.19	3
RG55	S 25° 23' 57.4"	E 30° 00' 21,3"	Dullstroom	57.83	0.54	14.53	10.12	0.2	4.86	7.42	1.79	1.27	0.13	0.03	0.01	0.03	0.02	1.76	58.13	15,52	117,72	5,7	51,38	353,94	219,26	163.48	136.1	3
RG60	S 25° 22' 55.0"	E 29° 57' 27,9"	Dullstroom	65.31	0.62	13.49	7.19	0.08	1.86	4.33	2.83	2.82	0.14	0.01	<0.01	0.02	0.03	1.28	55.61	19,8	180,79	7,91	85,72	524,09	246,25	109.69	49.73	3.32

RG62	S 25° 23' 07.0"	E 29° 57' 47,6"	Dullstroom	56.37	1.75	13.98	13.6	0.08	2.62	4.98	3.37	2.32	0.21	0.01	0.01	0.04	0.04	0.71	58.83	23,51	301,57	13,17	66,52	358,28	360,59	200.68	6.84	5.11
RG63	S 25° 23' 13.6"	E 29° 58' 01,8"	Dullstroom	55.38	0.75	14.72	10.1	0.19	4.83	8.45	2.25	1.51	0.13	0.03	0.01	0.03	0.02	1.69	57.97	21,68	132,57	7,08	53,97	331,85	241,62	187.09	161.68	3

Table 1

Rhyolitic MELTS options (Ghiorso & Gualda, 2015)				
MELTS parameters				
T (°C)	1400-800			
Liquidus (°C)	1346.88-1349.02			
Increments (°C)	10			
Pressure (bars)	2500			
Buffer	QMF			

Composition of initial melt	Fraction of melt remaining and proportions of crystallized phases at 2.5kbars, QMF			
	Upper crust			
z				
B1 (Barnes et al., 2010)	1132.62 (°C)	1072.62 (°C)	1052.62 (°C)	1032.62 (°C)
55.74 wt.% SiO_2	70% melt	50% melt	30% melt	20% melt
0.34 wt.% TiO_2	40.09% opx	45.74% opx	45.37% opx	45.18% opx
10.50 wt.% Fe_2O_3	10.04% feld	23.86% feld	31.28% feld	34.97% feld
11.85 wt.%MgO			8.51% qtz	12.25% qtz
6.50 wt.% CaO			3.74% cpx	5.54% cpx
0.98 wt.% K_2O				
	Lower crust			
	1149.02 (°C)	1099.02 (°C)	1029.02 (°C)	1009.02 (°C)
	70% melt	50% melt	30% melt	25% melt
	31% cpx	40% cpx	32% olivine	23% olivine
	62% opx	60% feld	9% cpx	23% cpx
			49% feld	48% feld
			10% spinel	6% spinel

Range of temperature are inferred from the previous work of Lenhardt and Eriksson (2012).
Upper crust assimilant used in the model is VG1 obtained from Buchanan et al. (2002).
qtz-Quartz, opx-Orthopyroxene, cpx-Clinopyroxene, feld-Feldspar

Table 2

Parental Composition	SiO_2 (wt.%)	Fe_2O_3 (wt.%)	Al_2O_3 (wt.%)	CaO (wt.%)	K_2O (wt.%)	MgO (wt.%)	% melt fractionation stage	Temperature (ºC)
low-Ti (LTI)	70.07	1.25	9.67	4.77	3.89	0.30	~75%	1021.29
B1	70.01	0.29	13.70	4.38	5.26	0.79	~85%	1001.25
B1 + ass.	70.04	0.65	12.90	6.29	1.57	1.97	~30%	1112.62
ADR	74.69	3.96	11.45	2.53	4.13	1.68	-	-

Table 3

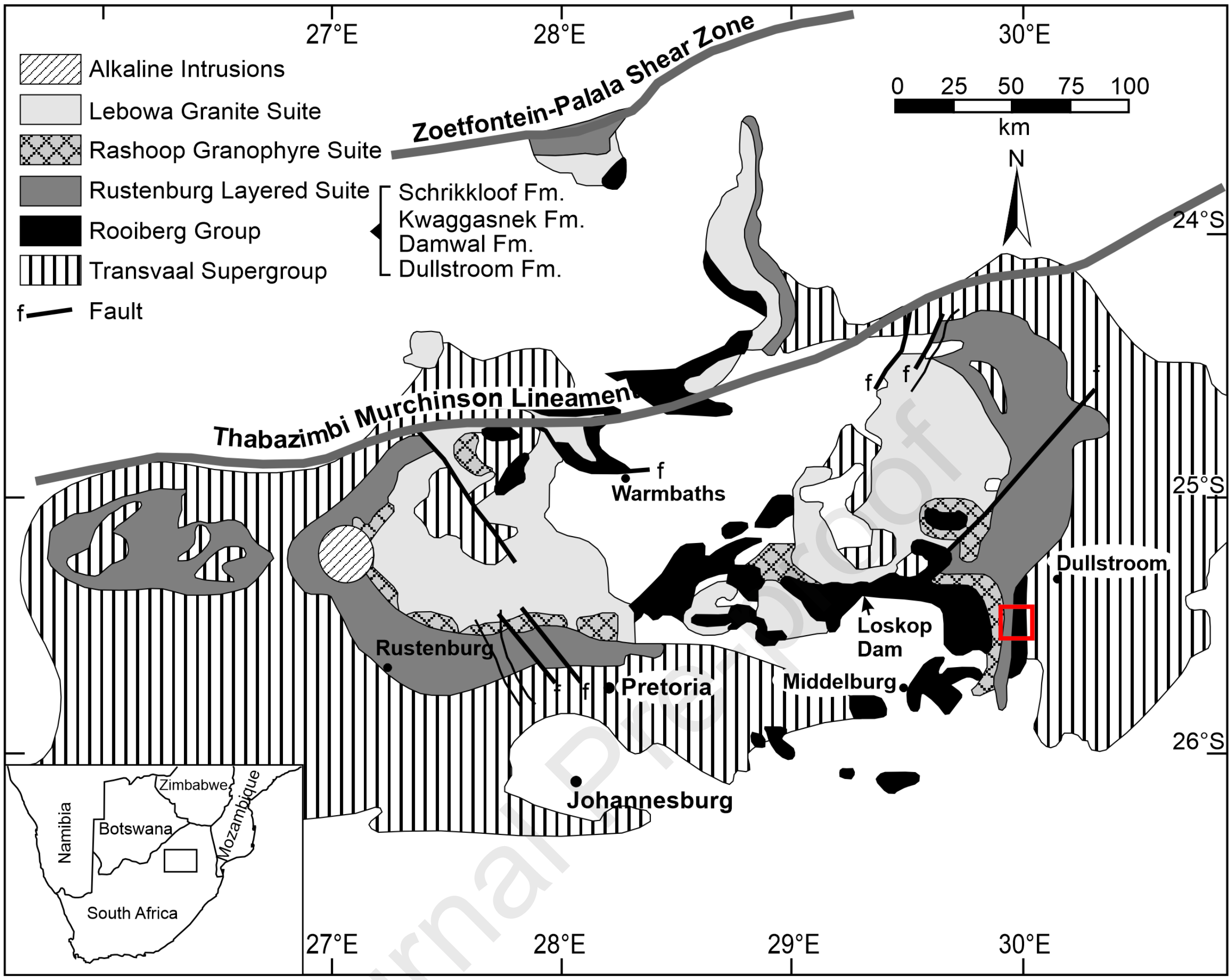

Alkaline Intrusions
Lebowa Granite Suite
Rashoop Granophyre Suite
Rustenburg Layered Suite
Rooiberg Group
Transvaal Supergroup
Fault
Schrikkloof Fm.
Kwaggasnek Fm.
Damwal Fm.
Dullstroom Fm.
Zoetfontein-Palala Shear Zone
Thabazimbi Murchinson Lineament
0 25 50 75 100
km
N
27°E
28°E
29°E
30°E
24°S
25°S
26°S
Warmbaths
Dullstroom
Loskop Dam
Rustenburg
Pretoria
Middelburg
Johannesburg
Zimbabwe
Namibia
Botswana
Mozambique
South Africa

Group	Formation	Thickness (m)	Main lithologies	Magma type
	Loskop	0-1000	Red shale, sandstone, conglomerate	
Rooiberg	Schrikkloof	200-3000	Rhyolite	Schrikkloof Low-Mg felsite
	Kwaggasnek	500-2500	Rhyolite, shale	Kwaggasnek Low-Mg felsite
	Damwal	1000-2500	Dacite, rhyolite	Bothasberg Low-Mg felsite; High Fe-Ti-P felsite
	Dullstroom	Up to 2000	Basalt to rhyolite	High Mg felsite; Low Ti basalt; High Ti basalt; Basal rhyolite
Pretoria (Upper part)	Rayton	1200	Quartzite, shale	
	Magaliesberg	300	Orthoquartzite	
	Silverton	600	Black shale	
	Dasport	80-95	Orthoquartzite	
	Strubenkop	105-120	Quartzite, shale	

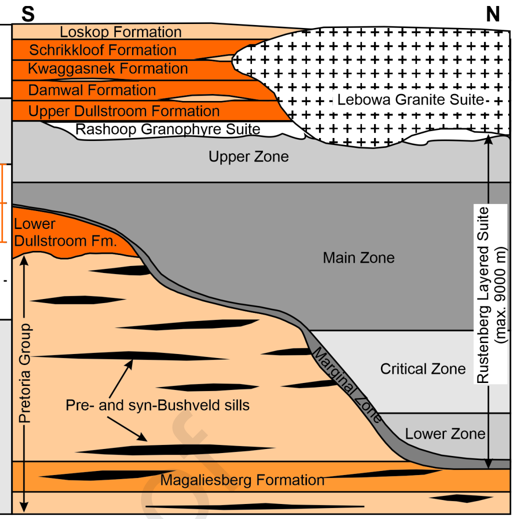

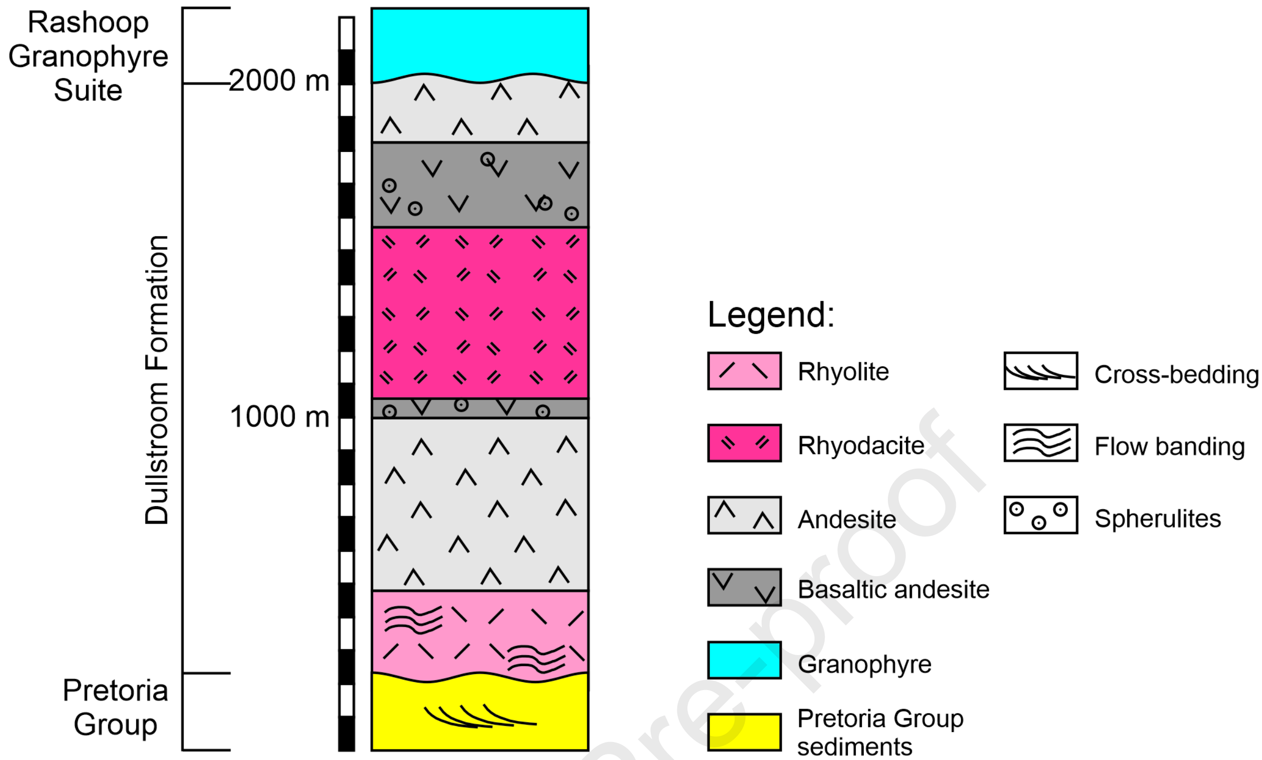
Rashoop Granophyre Suite
2000 m
Dullstroom Formation
1000 m
Pretoria Group
Legend:
Rhyolite
Rhyodacite
Andesite
Basaltic andesite
Granophyre
Pretoria Group sediments
Cross-bedding
Flow banding
Spherulites

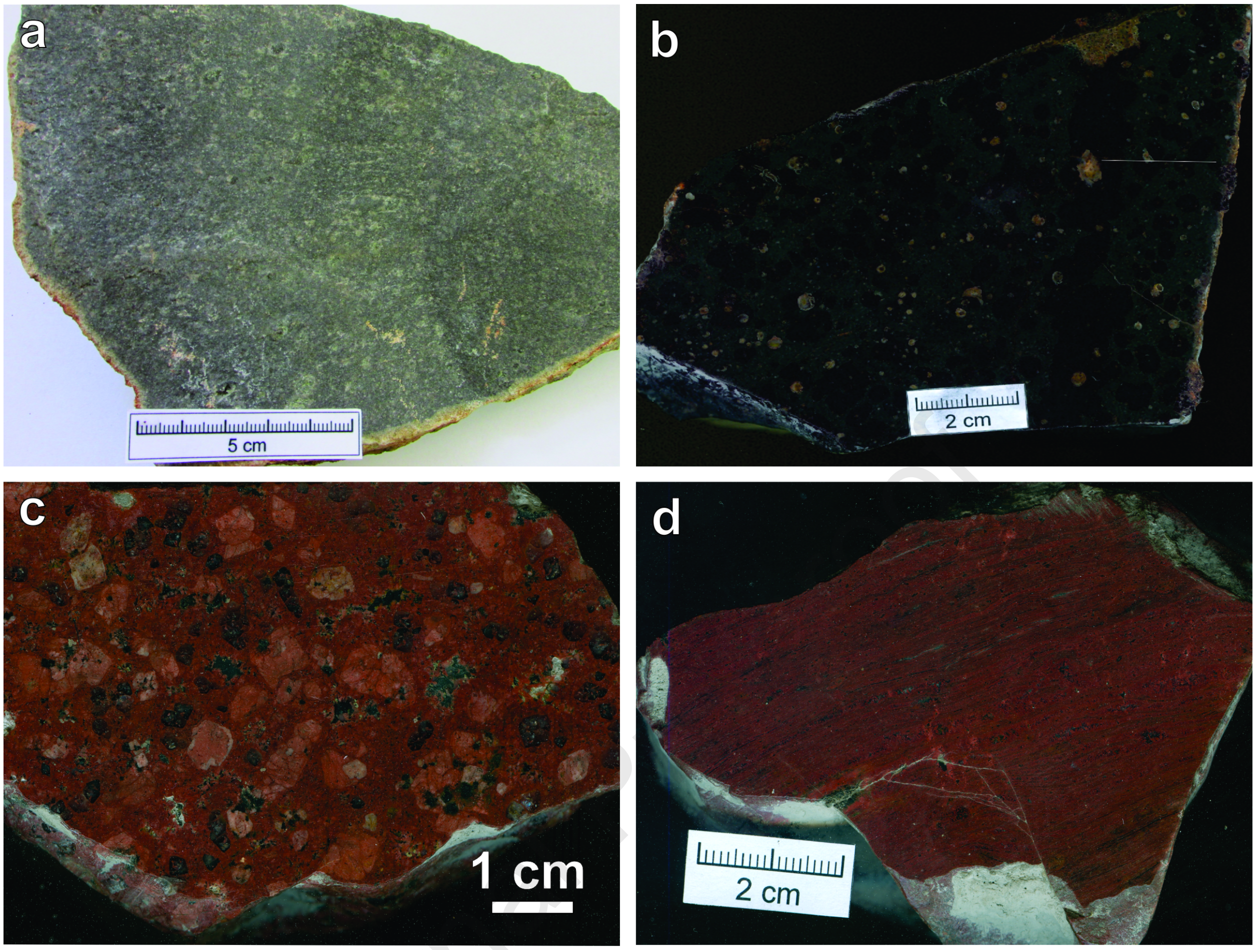

a
5 cm
b
2 cm
c
1 cm
d
2 cm

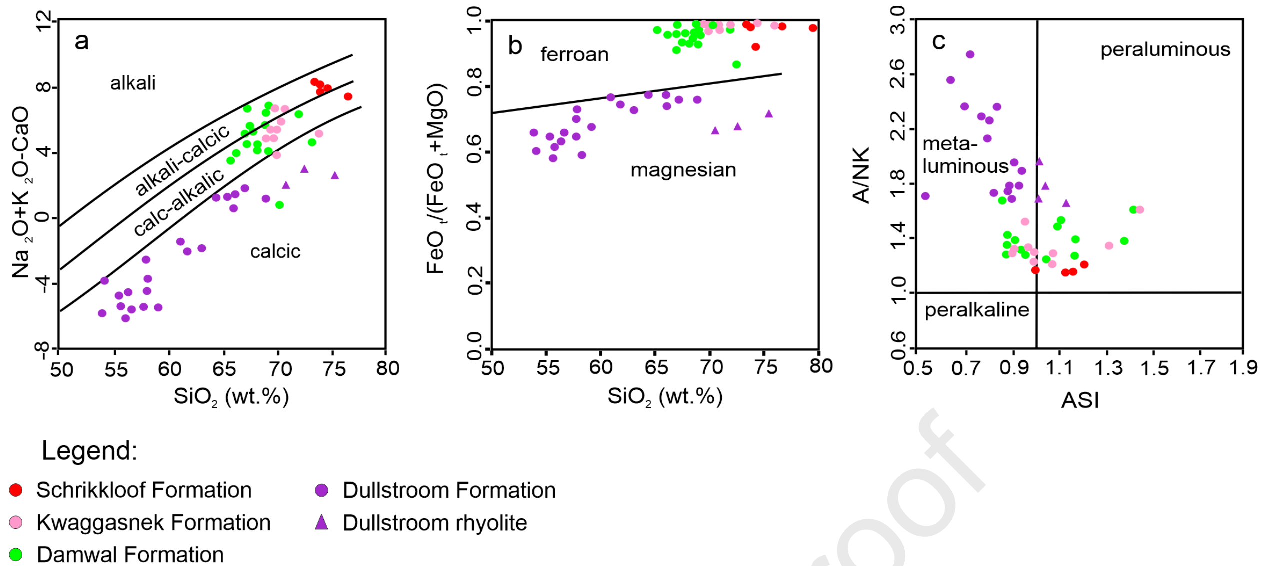
a
alkali
alkali-calcic
calc-alkalic
calcic
Na2O+K2O-CaO
SiO2 (wt.%)
b
ferroan
magnesian
FeOt/(FeOt+MgO)
SiO2 (wt.%)
c
peraluminous
meta-
luminous
peralkaline
A/NK
ASI
Legend:
Schrikkloof Formation
Kwaggasnek Formation
Damwal Formation
Dullstroom Formation
Dullstroom rhyolite

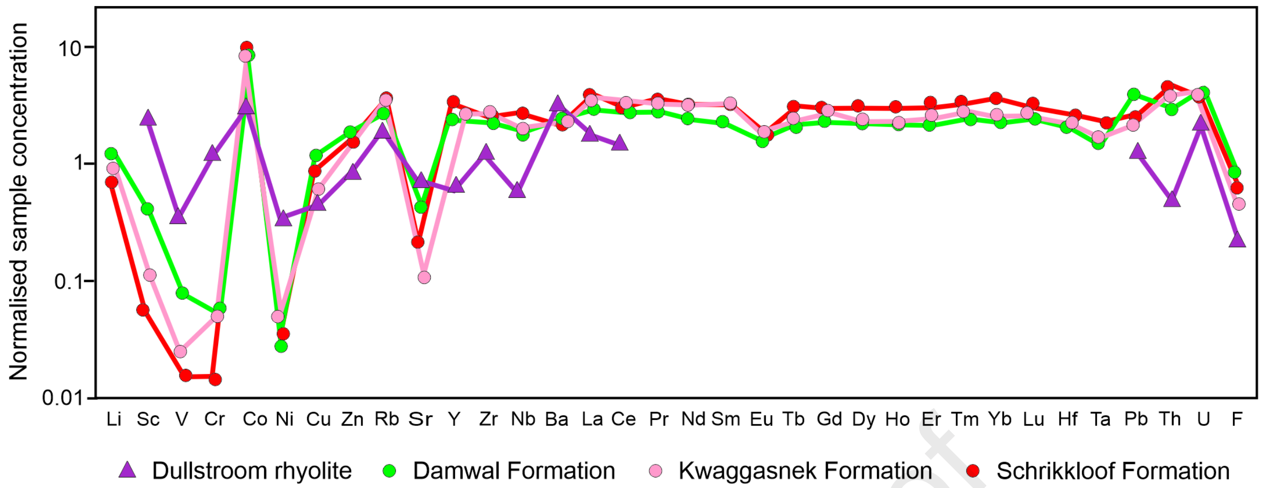
Normalised sample concentration
10
1
0.1
0.01
Li Sc V Cr Co Ni Cu Zn Rb Sr Y Zr Nb Ba La Ce Pr Nd Sm Eu Tb Gd Dy Ho Er Tm Yb Lu Hf Ta Pb Th U F
Dullstroom rhyolite
Damwal Formation
Kwaggasnek Formation
Schrikkloof Formation

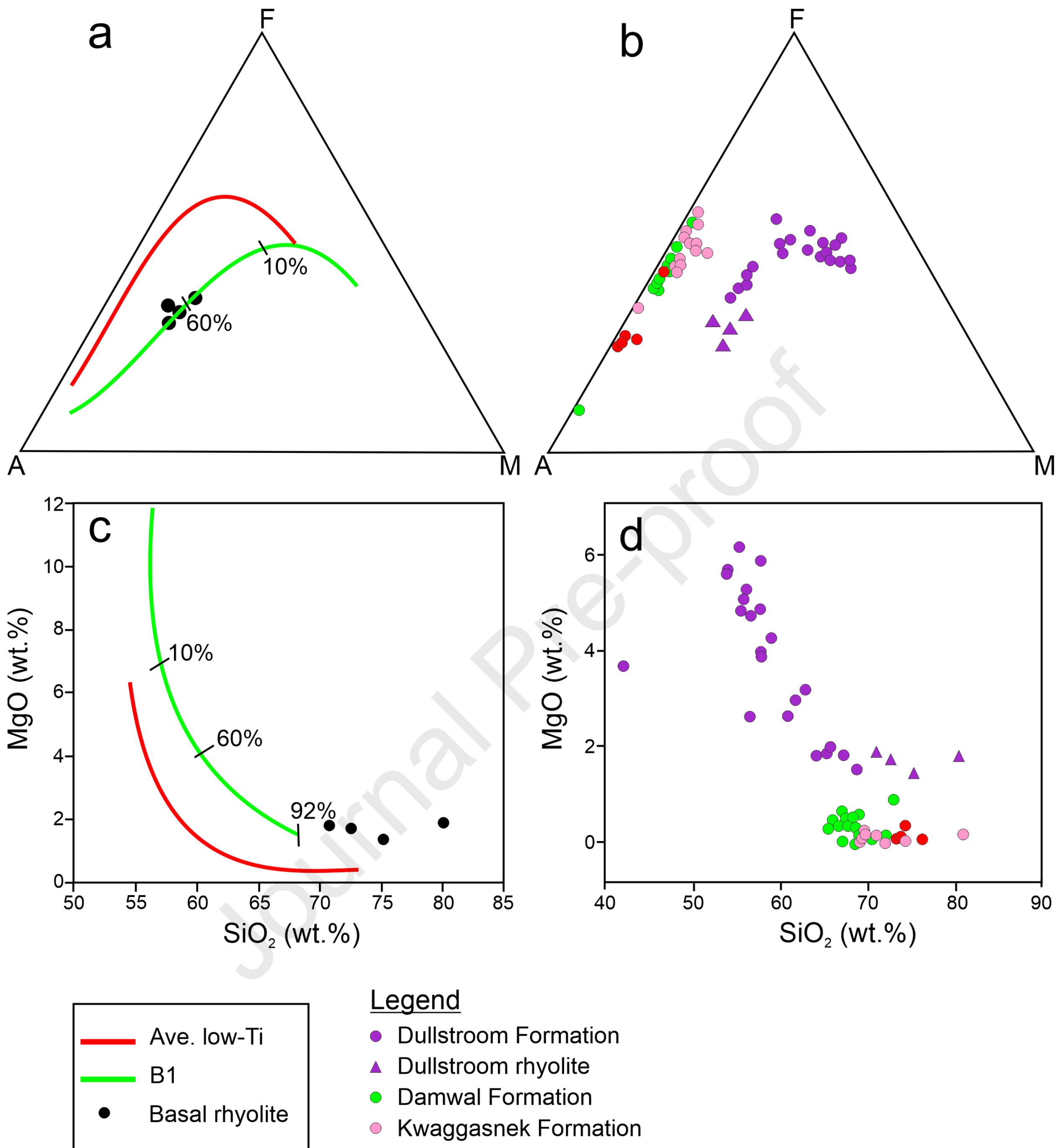
a
F
A
M
10%
60%
b
F
A
M
c
MgO (wt.%)
SiO2 (wt.%)
10%
60%
92%
d
MgO (wt.%)
SiO2 (wt.%)
Ave. low-Ti
B1
Basal rhyolite
Legend
Dullstroom Formation
Dullstroom rhyolite
Damwal Formation
Kwaggasnek Formation
Schrikkloof Formation

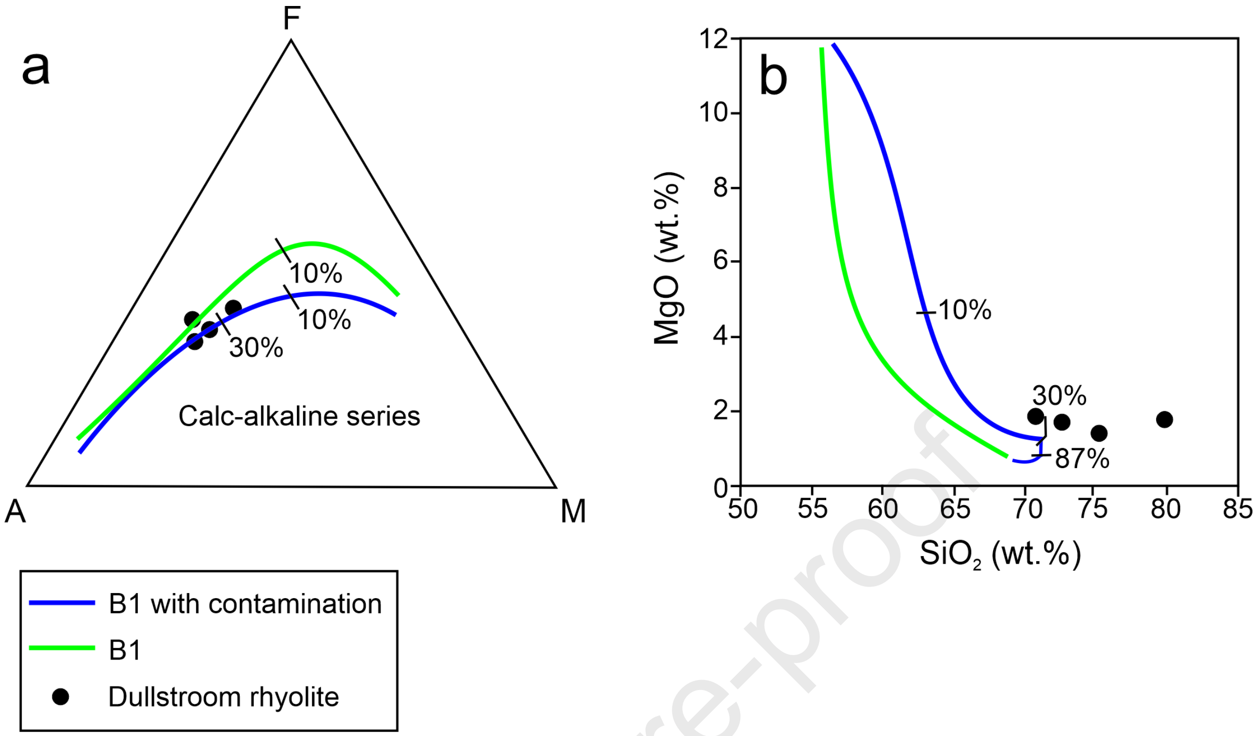

a
F
A
M
10%
10%
30%
Calc-alkaline series
B1 with contamination
B1
Dullstroom rhyolite
b
MgO (wt.%)
SiO2 (wt.%)
10%
30%
87%

Highlights

- The Rooiberg Group rocks exhibit both magnesian and ferroan rhyolites.
- The magnesian rhyolite is similar to the dominant mafic compositions in the Dullstroom Formation.
- MELTS show that the magnesian Dullstroom rhyolite formed from the B1 magma type.

I, the corresponding author on behalf of all the authors, have ensured that this work is genuine and is not submitted for publication or review in other places or platforms.